QUADRUPOLE MASS SPECTROMETER

A Thesis Submitted

In Partial Fulfilment of the Requirements

For the Degree of

MASTER OF TECHNOLOGY IN ELECTRICAL ENGINEERING

by

PRASHANT SAKSENA

to the

DEPARTMENT OF ELECTRICAL ENGINEERING

INDIAN INSTITUTE OF TECHNOLOGY, KANPUR

August, 1968

CERTIFICATE

Certified that this work on "Quadrupole Mass-Spectrometer" has been carried out under our supervision and has not been submitted elsewhere for a degree.

P. K. Ghosh

Dr. P. K. Ghosh 17-8-68
Assistant Professor
Department of Chemistry
Indian Institute of Technology,
Kanpur.

Dr. T. R. Viswanathan
Assistant Professor
Department of Electrical Engineering
Indian Institute of Technology,
Kanpur.

ACKNOWLEDGEMENT

The author is grateful to Dr. P. K. Ghosh for suggesting the problem. He also wishes to thank Dr. T. R. Viswanathan and Dr. P. K. Ghosh for their great interest, enthusiasm, critical appraisal and guidance throughout the work.

The lively atmosphere of the Post-graduate Laboratory, and the helpfulness of my colleagues, was extremely stimulating in carrying out the experimental work.

ABSTRACT

The design and development of a compact, simple and versatile mass spectrometer is discussed.

The mass spectrometer comprises 1) an ionizer, 2) analyser and 3) a Faraday Cup charge collector. The given sample in the vapour phase is injected into the ionizer, where mostly singly charged ions are generated and expelled as a collimated beam into the analyzer.

Ideally, the analyser is a symmetric array of four parallel hyperbolic rods, with the ion beam injected along the central axis of the array. A voltage of the form $\pm (U + V \cos \omega t)$ is applied to the rods, the diametrically opposite ones being connected together.

The spatial field distribution within the rod array leads to equations of motion of ion of the form of Mathieu Equation. Under predetermined value of U, V, U/V, and other random variables as the spatial momentum of the injected ions, the phase angle of r.f. at the instant when ions enter the analyser, the ions will either follow stable trajectories along the analyser-or be lost by going into unstable oscillations. Primarily, the magnitudes of U and V determine the mass selected in a given species of ions and U/V determines the controllable resolution of the analyser.

The mass scan is achieved by varying voltages U and V from low amplitude to high amplitude keeping U/V constant. Thus there exists

a one-to-one correspondence between the voltage and the mass selected. Short time (i.e. a time interval of one mass scan) stability of the voltages is extremely important. For a QMS of resolution 400 the empirical system requirements are:

1) Frequency stability, 1 in 1600.
2) Field radius tolerance, 1 in 1600.
3) Voltage U and V stability, 1 in 800.

This is the most important aspect of the development of a QMS.

The stable ions transmitted through the analyser are collected by the Faraday Cup and monitored by an Electrometer of sensitivity $\approx 10^{-14}$ Amps.

This system is extremely economical and well suited to residual gas analysis in a vacuum chamber.

TABLE OF CONTENTS

TABLE OF CONTENTS (Continued)

LIST OF FIGURES

CHAPTER 1

INTRODUCTION

Static mass spectrometers are characterised by time-invariant analyser fields, electric or magnetic, and only time the field conditions are changed is when a mass spectrum scan is desired. Dynamic mass spectrometers in contradistinction to static instruments involve time varying analyser field conditions, and mass separation is achieved by using different flight times or path stability of ions in the Analyser field.

Dynamic mass spectrometers have several important advantages e.g. in

1) precision determination of large masses.
2) applications where mass spectrometer is used in rockets for investigation of the composition of the upper atmosphere.
3) problems of Ultra High Vacuum technology where the analysis of residual gases down to extremely low pressures is required.
4) rapid and comprehensive mass analyses at medium resolution required for the investigation of combustion, and particulary explosion processes.
5) isotope separation.

The Quadrupole Mass Spectrometer (QMS) and its use as an isotope

separator was first reported by Paul et al. in 1953. This instrument operates without a magnet and uses a d.c. and r.f. field to achieve mass separation. The resolution of the instrument is controlled by the ratio of magnitudes of d.c. and r.f. voltages and is therefore, electronically controllable, unlike magnetic instruments where resolution is principally dependent on the width of the ion-beam. Mechanically, the design parameters of the quadrupole permit physically smaller instruments for a given resolution and this factor has been utilized for rocket-borne analysis of ionospheric charged particles (Brubaker, et al.). On the other hand, quadrupoles with resolution of the order of 10,000 have been constructed where high resolution have been necessary. The quadrupole has a large acceptance angle for ions and consequently a large transmission efficiency (Brubaker, 1961).

These features, and its relative in-expensiveness, make it perhaps the most versatile instrument available in the field of mass spectrometry today. It is with these facts and potentiality in view that the present project for the development of quadrupole mass spectrometer was undertaken. The design of electronic circuits which generate the necessary control voltages forms the major part of this thesis.

CHAPTER 2

QUADRUPOLE MASS SPECTROMETER THEORY

2.1 Principle of Operation

The Analyser portion of the QMS determines the ion path stability, and hence the mass selected. It consists of four precisely turned and rigidly mounted stainless steel (Type 304) rods. These are aligned, located parallel and equidistant to each other and also equidistant from a central axis. The d.c. and r.f. voltages are applied to the rods as shown in Figure 2.1. This generates an electrostatic field principally in the region enclosed by the four rods. The effect of fringe fields at the two ends of the Analyser is ignored for the following analysis.

If the rods are hyperbolic cylinders (in practice circular rods are used), the potential ϕ at any point (x, y) (Fig. 2.1) within the Analyser due to the electrostatic field is given by

$$\phi = (U + V \cos \omega t) \left(\frac{x^2 - y^2}{r_o^2} \right) \qquad 2.1$$

where,

U : magnitude of d.c. potential

V : peak amplitude of r.f. potential

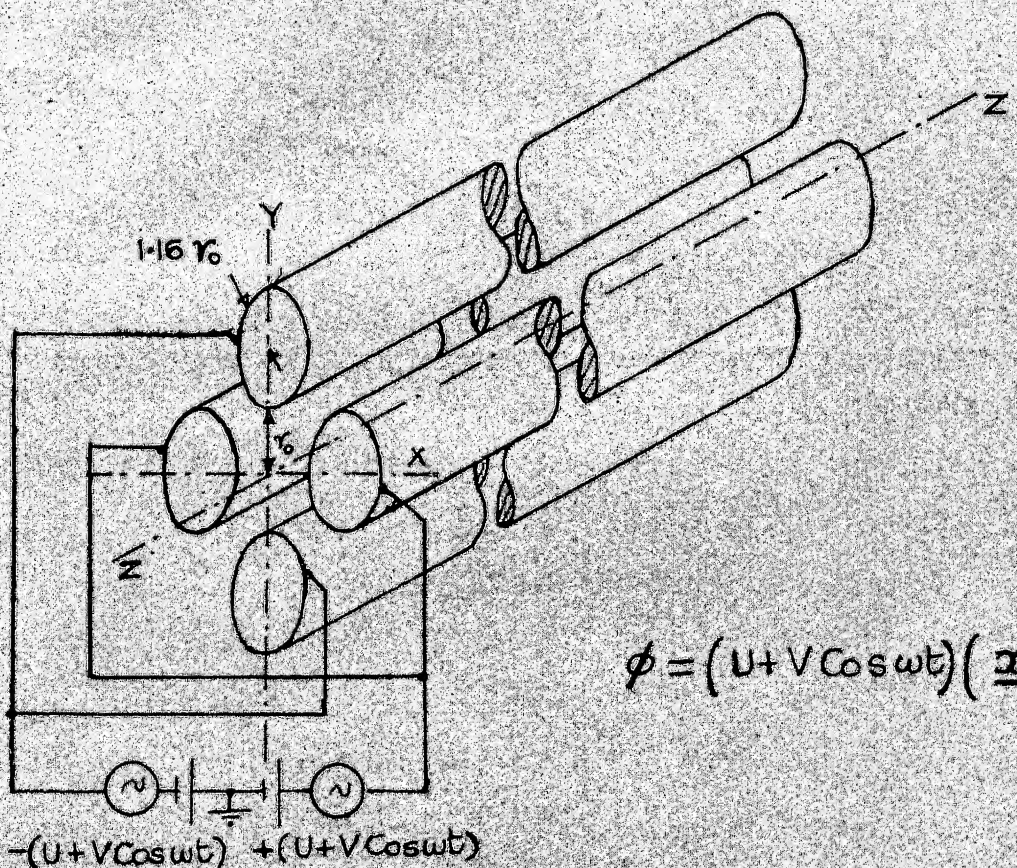

QMS ANALYSER

FIGURE - 2.1

ω : radio frequency in radians

r_o : 'field radius' shown in Fig. 2.1.

With circular rods, where rod diameter = 1.16 r_o this potential is only approximately generated.

When a singly charged ion (abbreviated to ion) of a given mass enters the Analyser, it is accelerated by the electrostatic field. We define

e : charge on an ion

m : number of atomic mass units (AMU) for a given ion

and let F_x, F_y and F_z represent the forces on the ion in the x, y and z directions respectively. Thus, we have

$$F_x = -e\frac{d\phi}{dx} = -e\,(U + V\cos\omega t)\left(\frac{2x}{r_o^2}\right) \qquad 2.2$$

$$F_y = -e\frac{d\phi}{dy} = +e\,(U + V\cos\omega t)\left(\frac{2y}{r_o^2}\right) \qquad 2.3$$

$$F_z = -e\frac{d\phi}{dz} = 0 \qquad 2.4$$

Hence, the equations of motion for any ion are

$$m\frac{d^2x}{dt^2} + e\,(U + V\cos\omega t)\left(\frac{2x}{r_o^2}\right) = 0 \qquad 2.5$$

$$m\frac{d^2y}{dt^2} - e\,(U + V\cos\omega t)\left(\frac{2y}{r_o^2}\right) = 0 \qquad 2.6$$

$$m\frac{d^2z}{dt^2} = 0 \qquad 2.7$$

Equation 2.7 states that the z-direction velocity of the ion is not altered. An ion will traverse the Analyser with a constant velocity in the z-direction equal to the initial velocity in the z-direction with which it entered the Analyser.

Defining ξ , a, q in the following parametric equations

$$\omega t = 2\xi \qquad 2.8$$

$$a = 8\, eU/(mr_o^2\omega^2) \qquad 2.9$$

$$q = 4eV/(mr_o^2\omega^2) \qquad 2.10$$

and changing the independent variable from t to ξ , gives

$$x'' + (a + 2q \cos 2\xi)\, x = 0 \qquad 2.11$$

$$y'' - (a + 2q \cos 2\xi)\, y = 0 \qquad 2.12$$

For any computation, the change in the independent variable must be accounted for with care. Taking the derivative of equation 2.8 gives

$$d\xi = \frac{\omega}{2}\, .dt \qquad 2.13$$

Equations 2.11 and 2.12 are of the form of Mathieu Differential Equation. However, the normal form of Mathieu Differential Equation is

$$x'' + (a - 2q \cos 2\xi)\, x = 0 \qquad 2.14$$

The technique of solving equation 2.14 has been treated by McLachlan (McLachlan, 1947). However, the solutions of equation 2.14 for a wide range of parameter a, q values and different initial conditions, may be obtained by numerical techniques on a digital computer using the Runge-Kutta's fourth order method (Froberg, 1964).

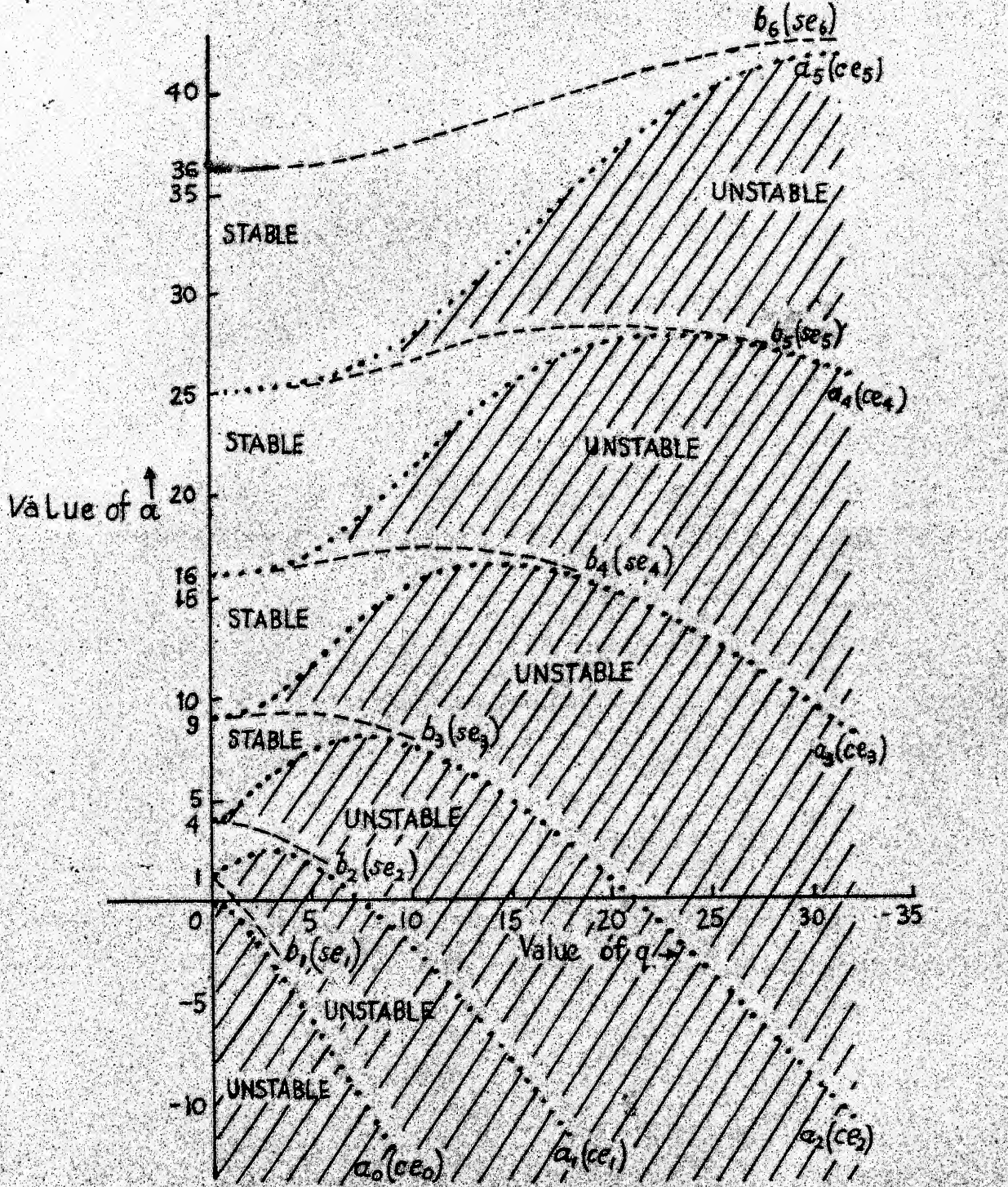

Stability chart for Mathieu functions of integral order (After McLachlan)

COMPLETE STABILITY CHART

FIGURE – 2.2

2.2 Stability Criteria

To define 'theoretical stability', based on the parameters a, q, we refer to Fig. 2.2 (After McLachlan, 1947). A trajectory is said to be stable if it is bounded with respect to time. If the amplitude of the trajectory exhibits a monotonously increasing trend, without being bounded with respect to time, it is unstable. In Fig. 2.2 regions of trajectory stability are shown unshaded on the a-q plane. The shaded regions indicate values of a, q which lead to unstable trajectories. These are the solutions for equation 2.14. The design of the Analyser is based on values of a, q at the apex of the stability chart in Fig.2.3 and also (1) the transverse momentum of the ion at the instant of injection into the Analyser (2) the phase angle of r.f. at the same instant. When the effects of these parameters are computed and known, the 'field radius', r_o is chosen so that the majority of ions have bounded trajectories not exceeding r_o. The length of the Analyser is kept long enough, so that the ions with a, q values in the unstable region have trajectories whose amplitudes exceed r_o-and these are not transmitted. It is obvious that, to keep the physical parameters of the QMS small, the stable region with lowest value of the parameters a, q must be chosen in Fig. 2.2.

It will be observed that equations 2.11 and 2.12 differ from equation 2.14 only in the sign of parameters a and q. For example, in equation 2.12 the sign of 'a' is negative, but in equation 2.14 the sign of 'a' is positive. By reflecting the complete stability chart of figure 2.2 on the q-axis and superposing it on the original complete stability chart gives the stability in both x and y directions. The region of practical interest

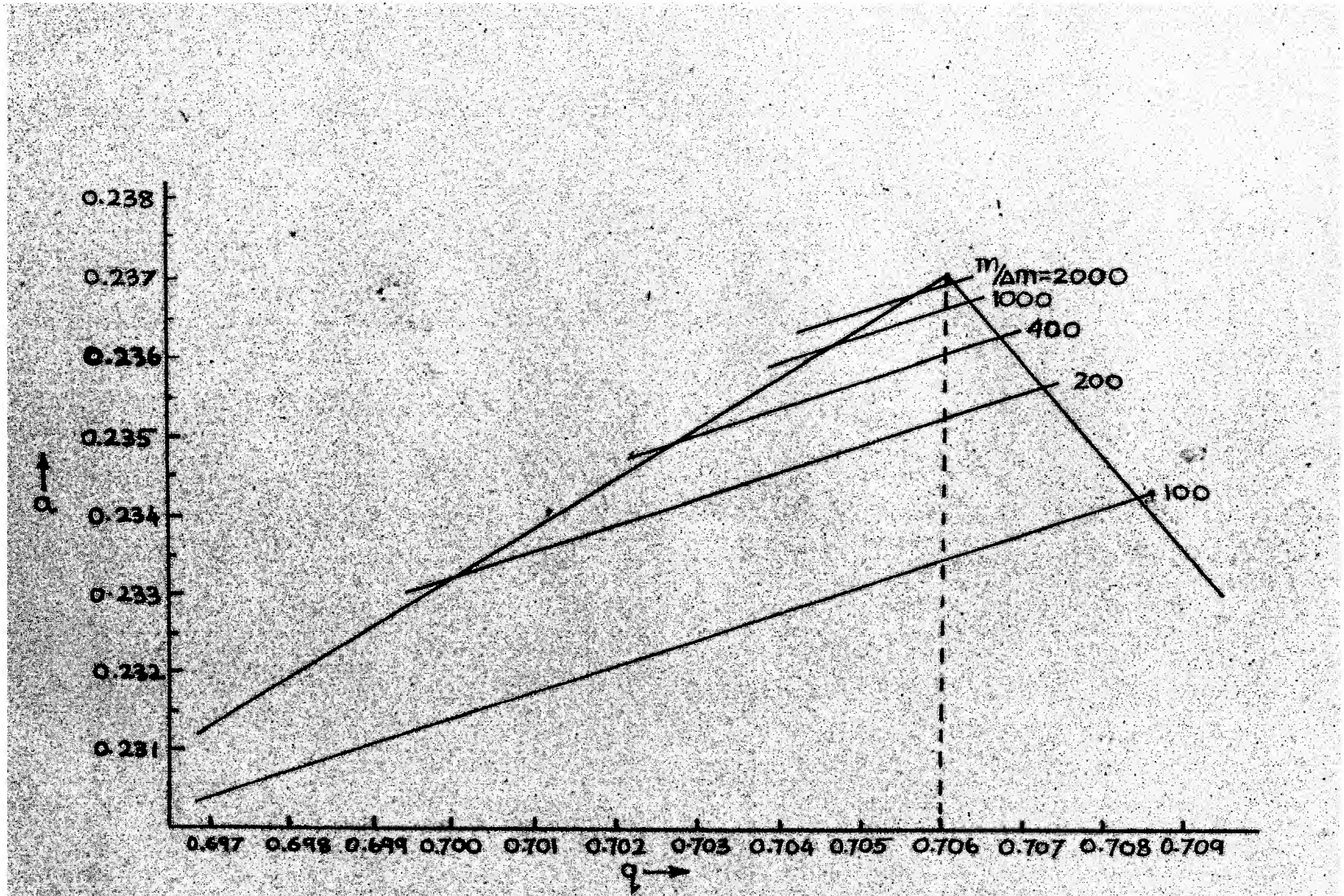

STABILITY CHART

FIGURE - 2.3

is magnified and shown in Fig. 2.3.

A straight line passing through the origin in Fig. 2.3 and having a segment within the stability region denotes a mass line for useful operation of the QMS. Theoretically, the heavier masses lie towards the origin of Fig. 2.3 and the lighter masses progressively farther away from it. The masses may be shifted continuously into and out of the stability region by varying the physical parameters of the QMS Analyser. This determines and distinguishes the transmitted ions from those that are not.

The following factors, at the instant of ion injection into the QMS Analyser, determine the maximum amplitude of ion trajectory in the x-z or y-z planes:

1) the transverse momentum
2) the phase of the r.f. voltage
3) the transverse displacement of the ion from the central axis, zz, in Fig. 2.1.

The increase of transverse momentum increases the maximum amplitude of the ion trajectory, without altering the time period of ion oscillation. It is interesting that the period of ion oscillation in the x-z plane is twice the r.f. period, whereas the period of ion oscillation in the y-z plane is the same as the r.f. period (Woodward and Crawford, 1964). The transverse displacement of the ion has negligible effect on the maxima of ion trajectories.

CHAPTER 3

QMS - GENERAL DESIGN CONSIDERATIONS

3.1 Resolution:

An important specification for any mass spectrometer is its resolution. It can be defined as the ability to clearly resolve two contiguous peaks of transmitted ion current. Generally speaking 'two peaks of equal height are said to be resolved when the valley between them is 10% of the height of either peak' (ULTEK, 1965).

Mathematically, resolution, R, is defined to be

$$R = m/\Delta m \qquad 3.1$$

where m is the centre mass and Δm the peak width of this centre mass. Figure 2.3 shows several mass lines, each corresponding to a different resolution. The increasing slope of the mass line diminishes the segment of the mass line lying in the stable region, and consequently improves the resolution of the QMS Analyser. It is incumbent that the values of parameters a and q must be tightly held within close tolerances if high resolution operation is desired. From the parametric equations 2.8, 2.9, 2.10 it is obvious that the physical parameters r_o, ω, U, V must be carefully controlled and should be stable. However, higher resolution leads to a reduction in the transmitted ion current through the Analyser and this calls for a more sensitive ion-current detector.

3.2 System and Analyser Specifications:

The specifications of the QMS Analyser used are given in Table 3.1.

TABLE 3.1

Desired resolution	400
Length of rods	7.6 cm.
Diameter of rods	0.3175 cm.
Field radius, r_o	0.1369 cm.

An empirical relation has been stated by Paul (Paul et al., 1958) for the required stability of the physical parameters. This is stated, and the practical requirements are listed, in Table 3.2.

TABLE 3.2

Stability or Accuracy of	Empirical Formula	Value	Percentage
U, V	$1 : 2x(m/\Delta m)$	1 : 800	± 0.125
ω, r_o	$1 : 4x(m/\Delta m)$	1 : 1600	± 0.0625
U/V (Calculated)			0.24

Paul has also stated an empirical relation for the required number of r.f. periods, N, for which the ions must remain in the Analyser field,

$$N \approx 3.5 \ (m/\Delta m)^{1/2} \qquad 3.2$$

Given that ions are injected into the analyser with an energy of 5eV, the velocity of an ion of atomic mass unit (AMU) 1 is 3.1×10^6 cm/sec. The length of the Analyser is 7.6 cms, and therefore time of ion residence in the Analyser is 2.45 μ sec. Choosing the r.f. period to be 1 μ sec. the value of N is 2.45. For AMU 10 the value of N is 7.75. From Paul's equation 3.2, the minimum value of N required is 70. However, Brubaker (Brubaker, 61) states that the number of periods of the applied r.f. required for an ion entering on the axis to reach its maximum amplitude is,

$$N = 1.11 (m/\Delta m)^{1/2} \qquad 3.3$$

It is assumed here that, for the Analyser used, resolution for AMU 1 - AMU 10 will be poor. The r.f. is chosen to be 1 MHz.

The equations 2.9, 2.10 are used to determine the required magnitudes of U, V at the apex (a = 0.23699, q = 0.70600) of the stability chart given in Figure 2.3. The calculated values are listed in Table 3.3.

TABLE 3.3

Magnitude of	A. M. U.		
	1	100	400
U, d.c. volts	0.0226	2.2650	9.0600
V, peak volts	0.1350	13.5000	54.00

3.3 Voltage Scan Versus Frequency Scan:

It will be seen from equations 2.9, 2.10 that any ion may be

brought within the stability region of Figure 2.3 provided a, q corresponding to a given mass lie in the stability region. This may be achieved by, keeping the other parameters constant, varying the frequency ω or the magnitudes of U and V (with U/V constant). From practical considerations, the latter method, i.e. a voltage scan is used. Thus each mass has a one-to-one correspondence with the magnitude of U or V selecting the mass. This permits calibration of the instrument directly in terms of the voltages. The resolution may be preset for a voltage scan if U/V is maintained constant.

CHAPTER 4

ELECTRONIC SYSTEM DESIGN

4.1 General Considerations:

In Chapter 3, it was explained that the QMS Analyser must be driven by two voltages of the form + (U + V Cos ω t) and - (U + V Cos ω t) in order to achieve a mass scan. As the r.f. and d.c. voltages of the required magnitude are varied from low amplitude (corresponding to the lowest mass) to high amplitude (corresponding to the highest mass) one mass scan is completed. If the given sample of ions traversing the QMS Analyser are monitored as one or more peaks of ion current at the detector their mass and relative abundance becomes known. If the given sample is not detected, the ions have masses outside the range of the mass scan. The electronic circuit must provide a means of varying U and V continuously and reproduceably, while keeping the ratio U/V (or resolution) a preset constant. This enables mass calibration in terms of the voltages, of which U is measured.

It was conceived that the required voltages may be generated in three different ways. All the three schemes incorporate a signal multiplier (Viswanathan, 1961). The signal multiplier has two inputs, a constant amplitude r.f. voltage and a monotonically increasing voltage (denoted MIV). The out-put of the signal multiplier is an r.f. whose

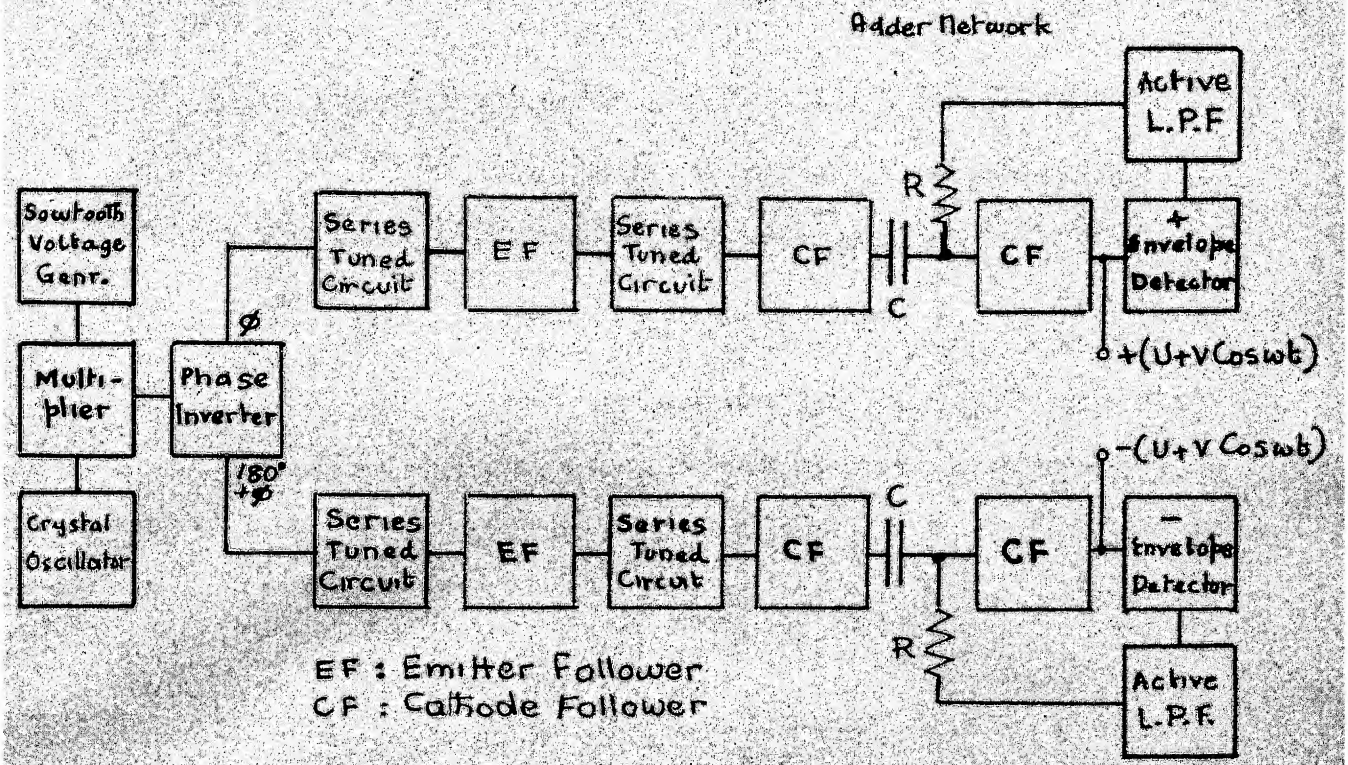

FIGURE – 4.1

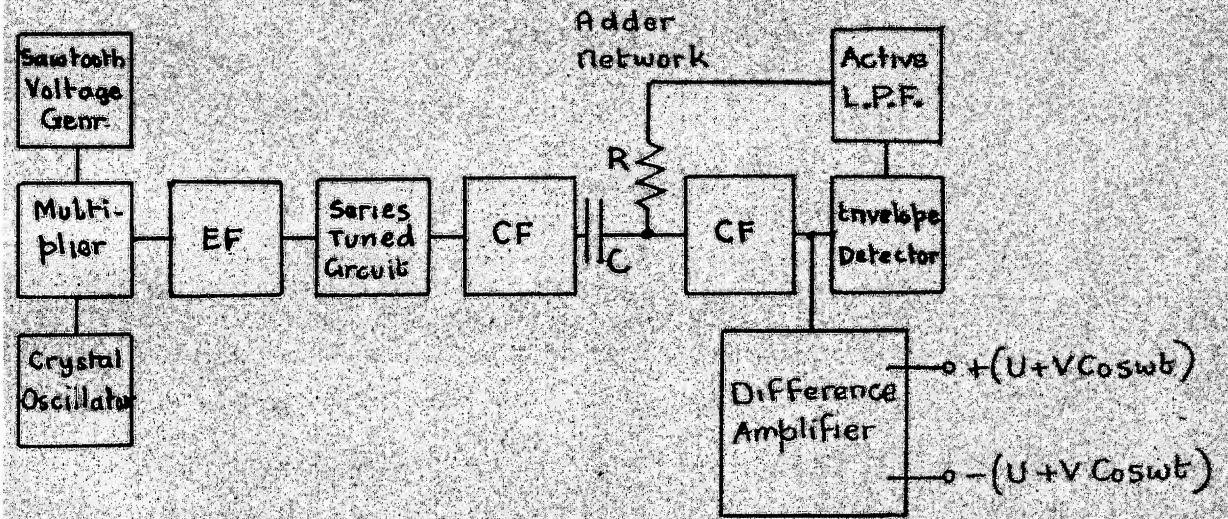

FIGURE- 4.2

amplitude at each instant is directly proportional to the MIV. In MANUAL mass scan the MIV is controlled by the variation of a potentiometer, whereas in AUTO mass scan the MIV is a sawtooth voltage of a time-interval as required for one mass scan.

4.2 Scheme A for Electronic Hardware:

It will be seen in Figure 4.1 that this approach provides linear amplification upto the output stage. The system is split into two chains after the phase-inverter. Unity gain cathode/emitter-followers act as buffer amplifiers between series tuned circuits providing the required voltage gain. At the output stage a voltage proportional to the r.f. voltage, V, is envelope-detected to derive the d.c. voltage, U, which is added to the voltage V itself, - thus the two chains generate the voltages $\pm$ (U + V Cos ωt). As this is an open-loop system, amplitude and phase stability will be poor. A cathode-follower using 12AT7 with a 30K load was observed to give frequency distortion for an output amplitude $\geq$ 8 volts peak.

4.3 Scheme B for Electronic Hardware

In Figure 4.2 a single chain identical to one of the two chains of Figure 4.1 generates the voltage (U + V Cos ωt). This signal is direct coupled to a balanced difference amplifier. The output of the difference amplifier at each of the two plates will be proportional to +(U+V Cos ωt) and -(U + V Cos ωt) respectively. The QMS Analyser rods must be at 0 volts under quiescent conditions, which fixes the plate potential of the difference amplifier to be 0 volts. The 6CB6 pentode is chosen for the difference amplifier and the 6CL6 power pentode is selected to act

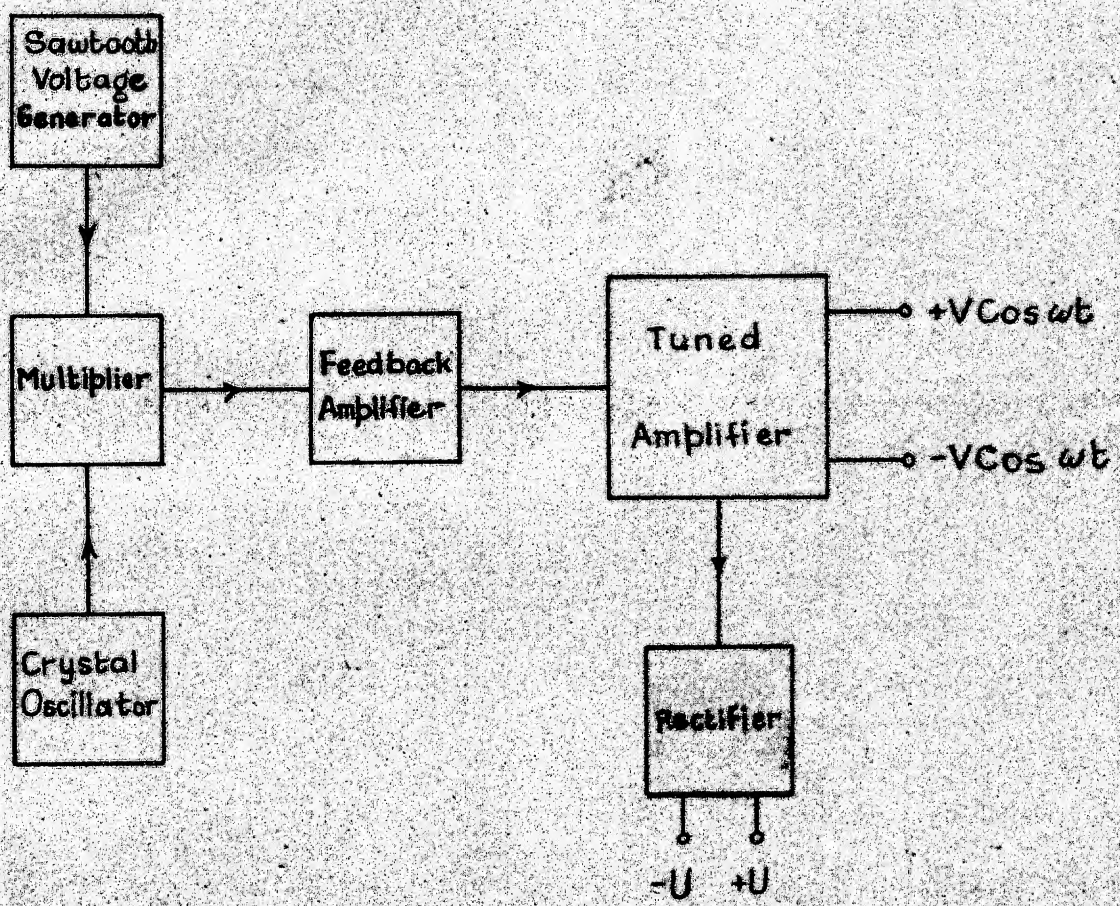

BLOCK DIAGRAM

FIGURE - 4.3

as a current source for the difference amplifier.

In the practical circuit d.c. drift was observed at the difference amplifier plates. This was attributed to

1) changes in VR tube voltage

2) plate resistor stability (AEC resistors have rated overall stability of 3%)

3) differential change in cathode emission of 6 CB 6's due to heater voltage changes.

4.4 Scheme C for Electronic Hardware:

Figure 4.3 outlines another method, which uses a centre-tapped secondary and bridge rectifier, to obtain the voltages $\pm (U + V \cos \omega t)$. This scheme has the highest short-time (i.e. time interval of one mass scan) stability. It is explained in detail in Chapter 7.

CHAPTER 5

CRYSTAL OSCILLATOR

5.1 General Considerations

It was stated in Chapter 3 that the voltages $\pm V \cos \omega t$ must be stable both in amplitude, V, and the frequency, ω. Therefore, a crystal-controlled oscillator at a frequency ω is required. The oscillator output voltage ($\approx$ 1 V r.m.s.) and the frequency (1 MHz) must be stable despite variations of the D^C supply voltage and ambient temperature. The requirement of the low amplitude output voltage from the oscillator can be conveniently achieved using an active device such as the conventional transistor or a Field-effect transistor (FET). The conventional transistor operating conditions and device parameters are known to be highly temperature dependent. In an FET, suitable biasing gives a quiescent operating point with a small temperature coefficient (Sevin, 64).

5.2 Oscillator Circuit Configuration

A simple equivalent circuit for the FET is shown in Fig. 5.1. This network, denoted as the active-device 3-pole in Fig. 5.2, is inter connected to the feedback 3-pole as shown. This configuration denotes a Colpitt's oscillator if y_4, y_5 are capacitive admittances and y_6 is an inductive admittance. The Colpitt's oscillator is used because it requires a single inductive element without tapping, and by using a crystal to replace the inductance higher frequency stability is achieved.

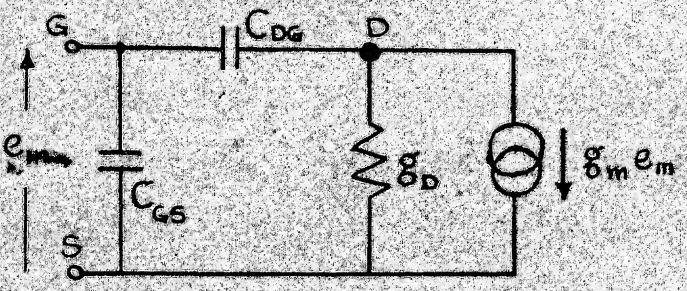

A simple equivalent circuit of the FET

FIGURE – 5.1

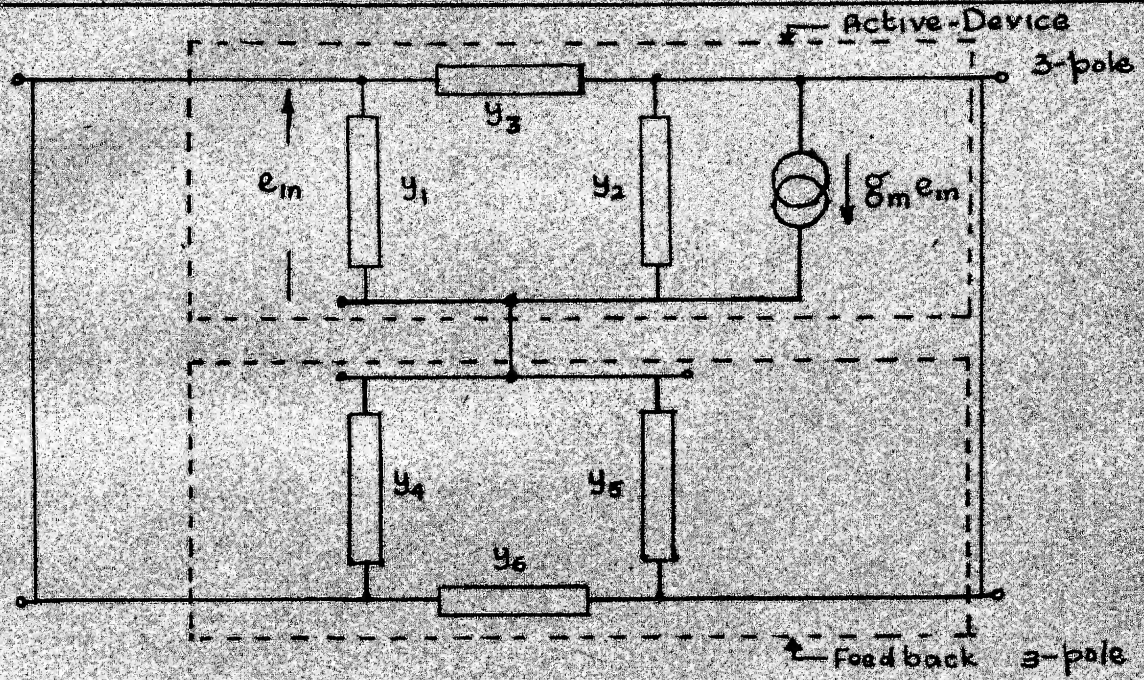

Interconnection of Active-device and Feedback network

FIGURE – 5.2

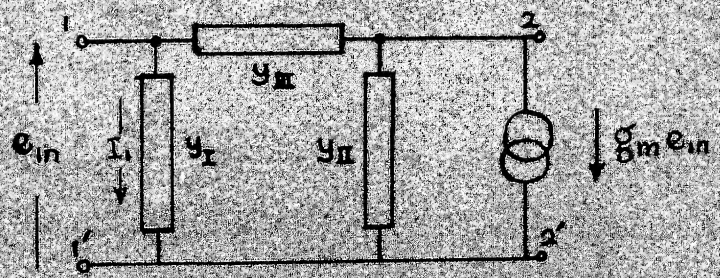

Combined equivalent circuit

FIGURE – 5.3

Fig. 5.3 represents the combined equivalent circuit, which is derived by adding the parallel admittances in Fig. 5.2 (Dosse, 1964) Let,

g_L : load conductance

g_D : incremental drain conductance

g_{LD} : total incremental drain conductance

then, $g_{LD} = g_L + g_D$ 5.1

and the symbols y_I, y_{II}, y_{III} in Fig. 5.3 be given by

$$y_I = j\omega(C_4 + C_{GS}) \stackrel{\text{def.}}{=} j\omega C_A \quad 5.2$$

$$y_{II} = j\omega C_5 + g_{LD} \stackrel{\text{def.}}{=} j\omega C_B + g_{LD} \quad 5.3$$

$$y_{III} = j\omega C_{DG} + \frac{1}{j\omega L} \stackrel{\text{def.}}{=} j\omega C_C + \frac{1}{j\omega L} \quad 5.4$$

In Fig. 5.3, if e_{in} is the voltage at terminals 11', then the current through y_I, which is I_1, is given by

$$I_1 = -g_m e_{in} \frac{y_I y_{III}}{y_I y_{II} + y_{II} y_{III} + y_{III} y_I} \quad 5.5$$

Also, $I_1 = y_I e_{in}$ 5.6

On combining equations 5.5, 5.6 we get

$$g_m y_{III} + y_I y_{II} + y_{II} y_{III} + y_{III} y_I = 0 \quad 5.7$$

On substituting equations 5.2, 5.3, 5.4 in equation 5.7 we get

$$\omega^2 L \left(C_C + \frac{C_A C_B}{C_A + C_B} \right) = 1 \quad 5.8$$

and $$g_{LD} = g_m \frac{C_B}{C_A} \quad 5.9$$

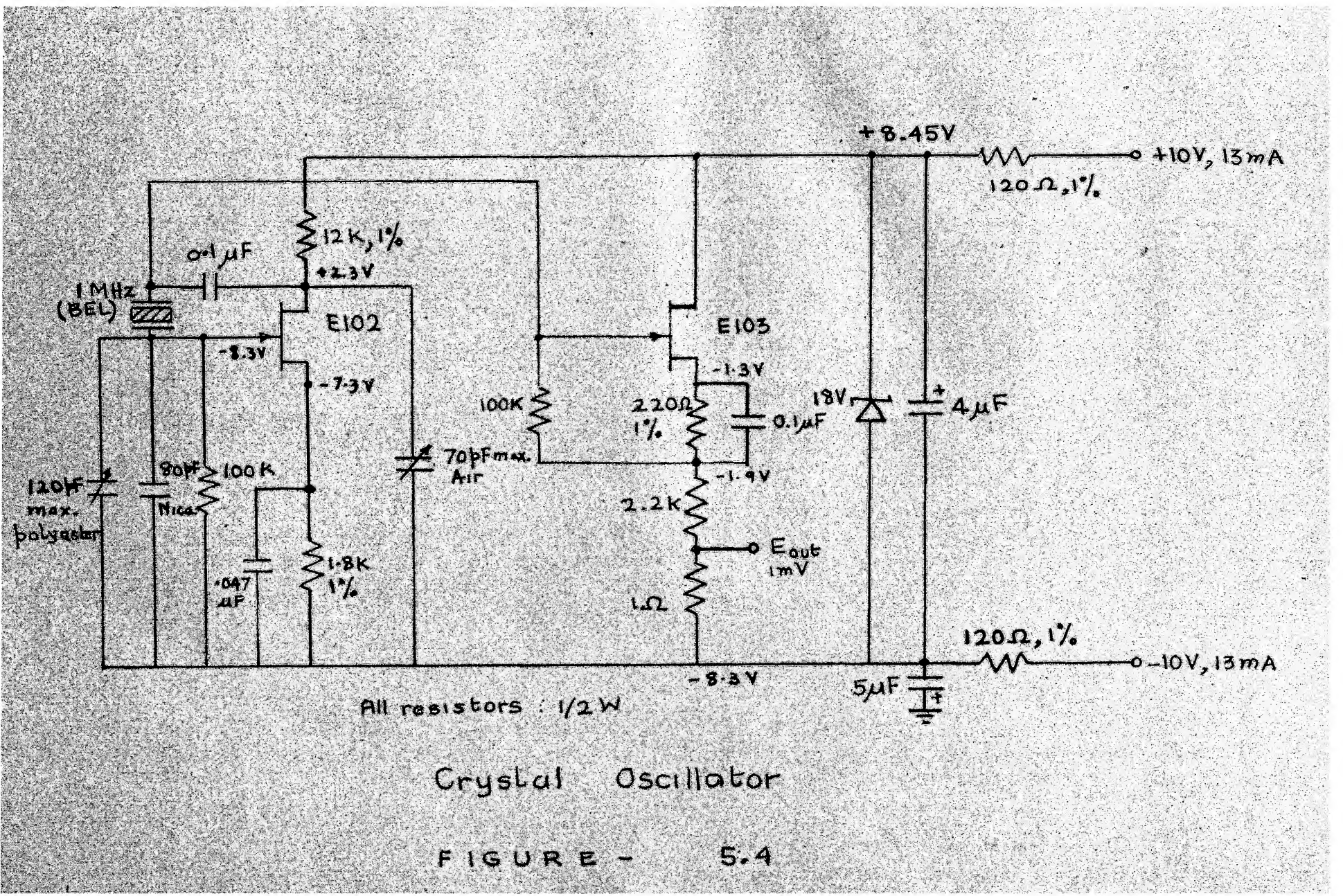

Crystal Oscillator

FIGURE - 5.4

Equation 5.8 gives the condition for frequency of oscillation and the load resistance can be calculated from equation 5.9.

5.3 Choice of Circuit Parameters

Given that $C_{DG} = C_{GS} = 4$ pF and letting $C_4 = 200$ pF, $C_5 = 50$ pF the value of L, calculated from equation 5.8 at 1 MHz, is 568 μH. A 1 MHz crystal is used as the inductive element, y_6, in Fig. 5.2.

For the FET type E102, we choose an operating point such that $I_{DQ} = 0.5$ mA, $V_{DS} = 11$ V, $g_m = .600$ m$\mho$ on the basis of linearity of voltage swing at the operating point.

The measured incremental drain resistance for the FET at the operating point is 20 KΩ. From equation 5.9 the required value of g_{LD} is .150 m$\mho$. Now $g_D = .05$ m$\mho$, hence equation 5.1 gives $g_L = .10$ m$\mho$. The required value of load resistance is 10 KΩ.

5.4 Source Follower

A source follower using FET type E103 is used to act as a buffer amplifier between the crystal oscillator and its load. The design is based on the low-frequency, large-signal graphical method of analysis of a vacuum tube cathode follower (Ryder, 1964).

The output impedance of the source follower is $1/g_m \approx 1000\Omega$. The load-resistor is split to

1) provide self-bias and
2) to give a r.f. signal from 1Ω impedance, which is used for the signal multiplier described in the next Chapter.

A zener-diode voltage regulator is incorporated in the circuit (Fig. 5.4) to keep the supply voltage constant.

The frequency stability of this circuit, measured over a time interval of 90 minutes is given in Table 5.1.

TABLE 5.1

FREQUENCY STABILITY OF THE OSCILLATOR

Ambient temperature : 37.5°C

Oscillator voltage : 1.5 V r.m.s.

Time, Hours	Frequency, Hz
1130	999, 979
1140	999, 980
1150	999, 979
1203	999, 980
1210	999, 980
1230	999, 979
1240	999, 979
1250	999, 980
1300	999, 979

This shows that the frequency stability during the test duration is better than 1 part in 10^6.

CHAPTER 6

SIGNAL MULTIPLIER AND FEEDBACK AMPLIFIER

6.1 Multiplier Theory

The exponential characteristic of a silicon p-n junction is exploited to achieve analog multiplication (Viswanathan, 1961). The principle of operation is briefly discussed here.

The forward voltage V across a diode and the forward current I through it are related by

$$I = I_s \ (e^{\gamma V} - 1) \qquad 6.1$$

where I_s is the theoretical value of the reverse saturation current. Defining,

q : electronic charge

K : Boltzmann constant

T : the absolute temperature

and n : a constant nearly equal to unity

then $\gamma = q / n K T$ 6.2

If the diode is operated such that $V \gg \frac{1}{\gamma}$, equation 6.1 may be written as

$$I = I_s \ e^{\gamma V} \qquad 6.3$$

Taking the first derivative of equation 6.3 with respect to V gives

$$g = \frac{dI}{dV} = \gamma I \qquad 6.4$$

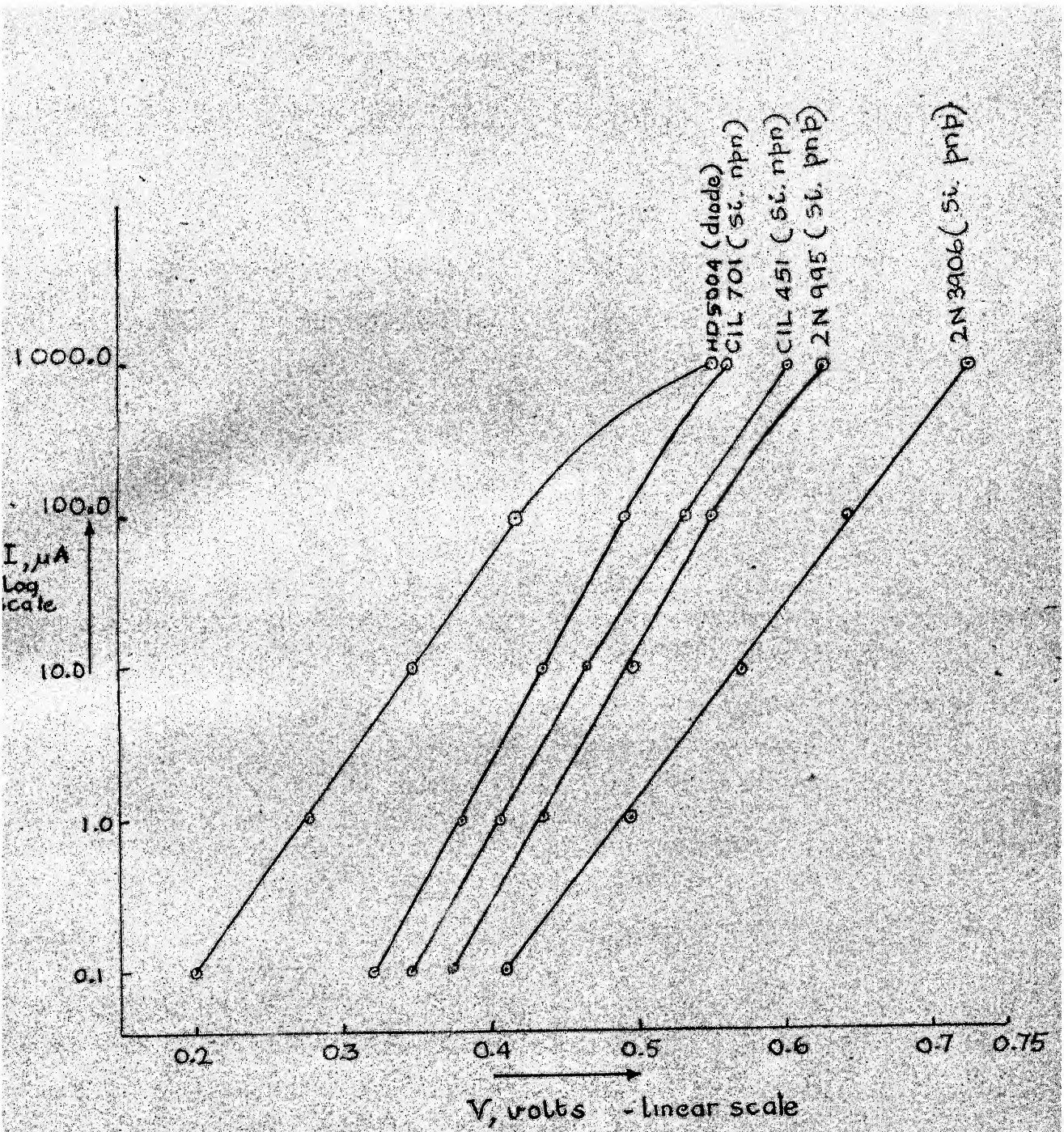

Log I vs. V characteristics for E-B Junction

FIGURE - 6.1

where g is the incremental input conductance of the diode. Instead of a diode, the emitter-base junction of a common - base transistor is used. Let a current, I, which is derived from the sawtooth voltage be forced into the emitter. This makes the conductance of the emitter-base diode directly proportional to the current I.

The r.f. signal, v, from a voltage source of 1 ohm impedance is now a-c coupled to the emitter of the transistor (Fig. 6.4). It can be seen that the r.f. collector current is directly proportional to the product of current I and voltage v. As I is linearly increased the r.f. collector current, and hence voltage, also increase linearly. The collector load is a tuned transformer, which blocks dc, while giving a linearly increasing r.f. at the secondary side. This r.f. signal is the input to the feedback amplifier, which consists of a difference amplifier in which negative feedback has been incorporated for obtaining good linearity and stability.

6.2 Selection of a Transistor for the Multiplier

Equation 6.1 is the ideal current (I)-voltage (V) law for a p-n junction, which is only approximated by the physical device. In the region of practical operation of the device, the log I vs. V characteristic must be linear. This assures a good linearity of the analog multiplication. With this point of view, the log I vs. V characteristic for the emitter-base junction of several transistors is measured and plotted in Fig. 6.1.

The 2N995 transistor is chosen for its good linearity in the current range 0.1-100 μA. It has an f_T of 100 MHz.

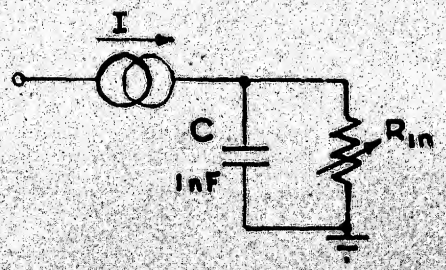

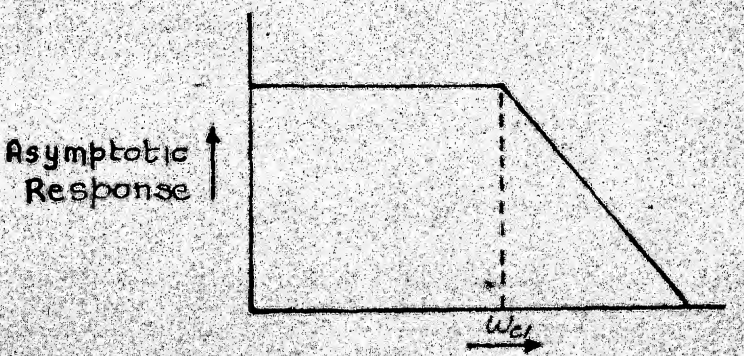

R_{in} = 750Ω for I = 80μA

= 60KΩ for I = 1μA

Input circuit for low frequency

FIGURE - 6.2

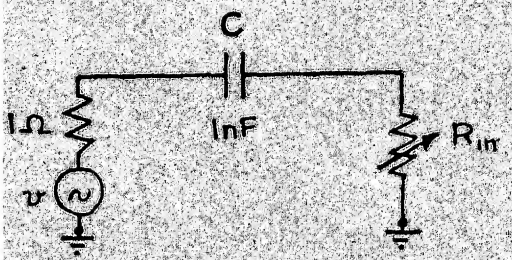

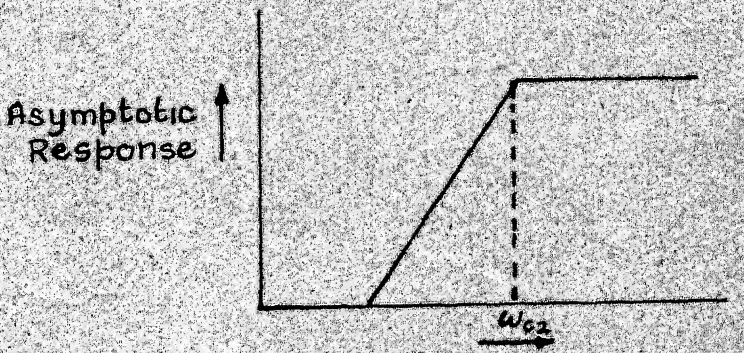

R_{in} = 750Ω for I = 80μA

= 60kΩ for I = 1μA

Input circuit for high frequency

FIGURE - 6.3

6.3 Multiplier Circuit Design

It has been shown that the incremental conductance of the emitter-base junction of the common-base transistor is proportional to the current I. To determine this conductance for the 2N995 transistor, we need the value of γ - which is given by the slope of the log I vs. V plot in Fig. 6.1. The value of γ^{-1} is 60 m V. The current, I, is varied from 1 μA to 80 μA, which varies the incremental resistance of the emitter-base diode from 60K Ω to 750 Ω.

Fig. 6.2 shows the equivalent circuit for low-frequencies at the input to the multiplier. The current, I, is a sawtooth which increases from a minimum to maximum in 5 seconds. This is the time interval for one mass scan of the QMS.

The response of this low pass filter must have a cross-over frequency, ω_{c1}, which allows transmission of the fundamental and harmonic frequency components of I. Choosing $\omega_{c1} = 10^4$ rad./sec. as the lowest cross-over frequency, for $R_{in} = 60$ K Ω, gives C ≈ .001 uF.

Fig. 6.3 shows the equivalent circuit for high-frequencies at the input to the multiplier. This is a high-pass network whose input is the voltage source, v, at 1 MHz. For this network, the highest cross-over frequency, ω_{c2}, for $R_{in} = 750$ is 212 KHz. This frequency is more than 2 octaves below 1 MHz, which ensures almost unity transmission of the high-pass network at 1 MHz.

In the multiplier circuit, an I.F. transformer is used (with the can removed to increase its Q) as the collector load, as shown in Fig.6.4. With the secondary open-circuited the impedance of the primary at the

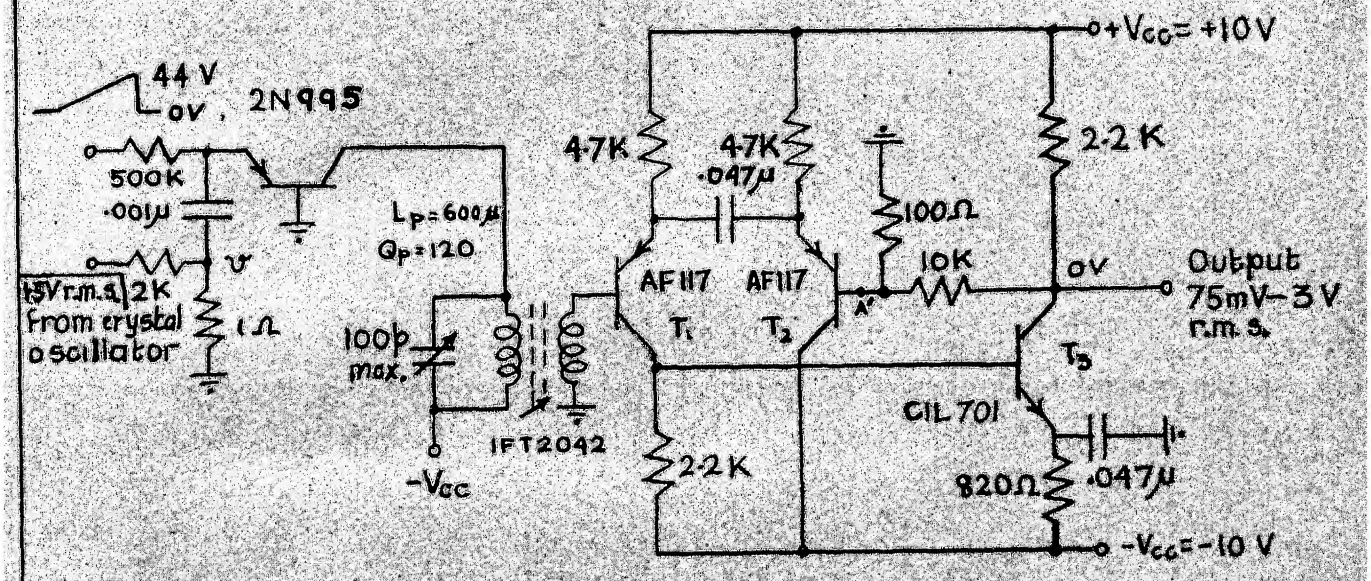

All resistors : 1/2 W, 5%.

Amplifier Gain = 100

MULTIPLIER AND FEEDBACK AMPLIFIER

FIGURE – 6.4

resonant frequency, calculated for the transformer parameters shown in Fig. 6.4 is 450 KΩ. If an r.f. signal of 1 m V peak is applied at the input to the multiplier, the r.f. collector voltage when the incremental input conductance is 750 Ω, is 0.6 volts. With a primary to secondary turns ratio of 15:1, the voltage induced in the open-circuited secondary of IFT 2042 is 40 mV peak.

This signal is applied to a feedback amplifier to give a voltage gain of 100 at 1 MHz.

6.4 Feedback Amplifier Design

The circuit shown in Fig. 6.4 consists of a difference amplifier and a common-emitter amplifier. Negative feedback is applied to the difference amplifier to achieve good linearity and stability. The gain calculations for the amplifier are as follows.

An emitter current of approximately 2 mA flows in each of the AF 117 (Ge) transistors of the difference amplifier. This gives an $r_e \approx 13\Omega$ for the AF117. Also, with the d.c. conditions shown, $r_e \approx 15\Omega$ for the CIL 701 (Si)- which gives $h_{ie} = 1.5\ K\Omega$.

If we break the loop at A', and inject a unit voltage signal into the base of T_2, the voltage gain at the collector of T_1 is 34.3. The loop gain, M, which is the voltage which appears at A' is 41.8. As the loop gain is large compared to unity, the gain of this amplifier with feedback is the reciprocal of the feedback factor. The voltage gain with feedback is 100.

The input impedance, Z_{in}, of the amplifier without feedback is

2. $h_{ie} \approx 5.2$ KΩ. Hence the input impedance with feedback, Z_{inf}, is

$$Z_{inf} = (1 - M) Z_{in} \qquad 6.5$$

$$= 218 \text{ K}\Omega .$$

The maximum undistorted output of the amplifier is 3 V r.m.s.

TABLE 6.2

MULTIPLIER LINEARITY MEASUREMENT

DC Input, volts	R F Amplitude r.m.s. mVolts	Ratio DC/RF	
		Value	Value normalised with respect to 16.
0	75	0	0
2	130	15.38	.961
4	230	17.40	1.088
6	340	17.65	1.104
8	460	17.40	1.088
10	570	17.55	1.098
12	700	17.15	1.071
14	820	17.06	1.067
16	960	16.67	1.040
18	1080	16.67	1.040
20	1220	16.38	1.025
22	1360	16.18	1.010
24	1500	16.00	1.000
26	1630	15.95	.997
28	1790	15.64	.978
30	1920	15.64	.978
32	2080	15.38	.961
34	2230	15.25	.953
36	2370	15.20	.950
38	2520	15.08	.943
40	2700	14.80	.925
42	2850	14.75	.922
44	3000	14.65	.916

CHAPTER 7

TUNED AMPLIFIER AND BRIDGE RECTIFIER

7.1 Introduction

It was shown in Chapter 6 that analog multiplication of a sawtooth voltage and an r.f. voltage gives a linearly increasing r.f. voltage. This r.f. voltage is the input to a tuned amplifier. The secondary winding of the tuned amplifier is centre tapped to give the voltages $\pm$ V Cos ωt. A bridge rectifier across the secondary winding gives the d.c. voltages $\pm$ U, which at each instant of time are proportional to the amplitude of the r.f. voltage, V. The d.c. voltage is applied to the QMS Analyser rods through low pass filters.

7.2 Tuned Amplifier Design

A type 807 beam power tube is chosen for the tuned amplifier on the basis of its low plate resistance and maximum plate voltage rating of 600 V. In the bridge rectifier on the secondary side, semiconductor diodes are used for a low amplitude voltage scan. For a high amplitude voltage scan, thermionic diodes with regulated heater supply are used. The choice of the diodes is based on the voltage breakdown rating, and low interelectrode or junction capacitance.

Fig. 7.1 shows the circuit used to generate the voltage $\pm$ (U + V Cos ωt). The tuned amplifier has an unbypassed cathode resistor for negative feedback and its plate load is a tuned-primary, tuned-secondary transformer. The input voltage of the tuned amplifier is a linearly

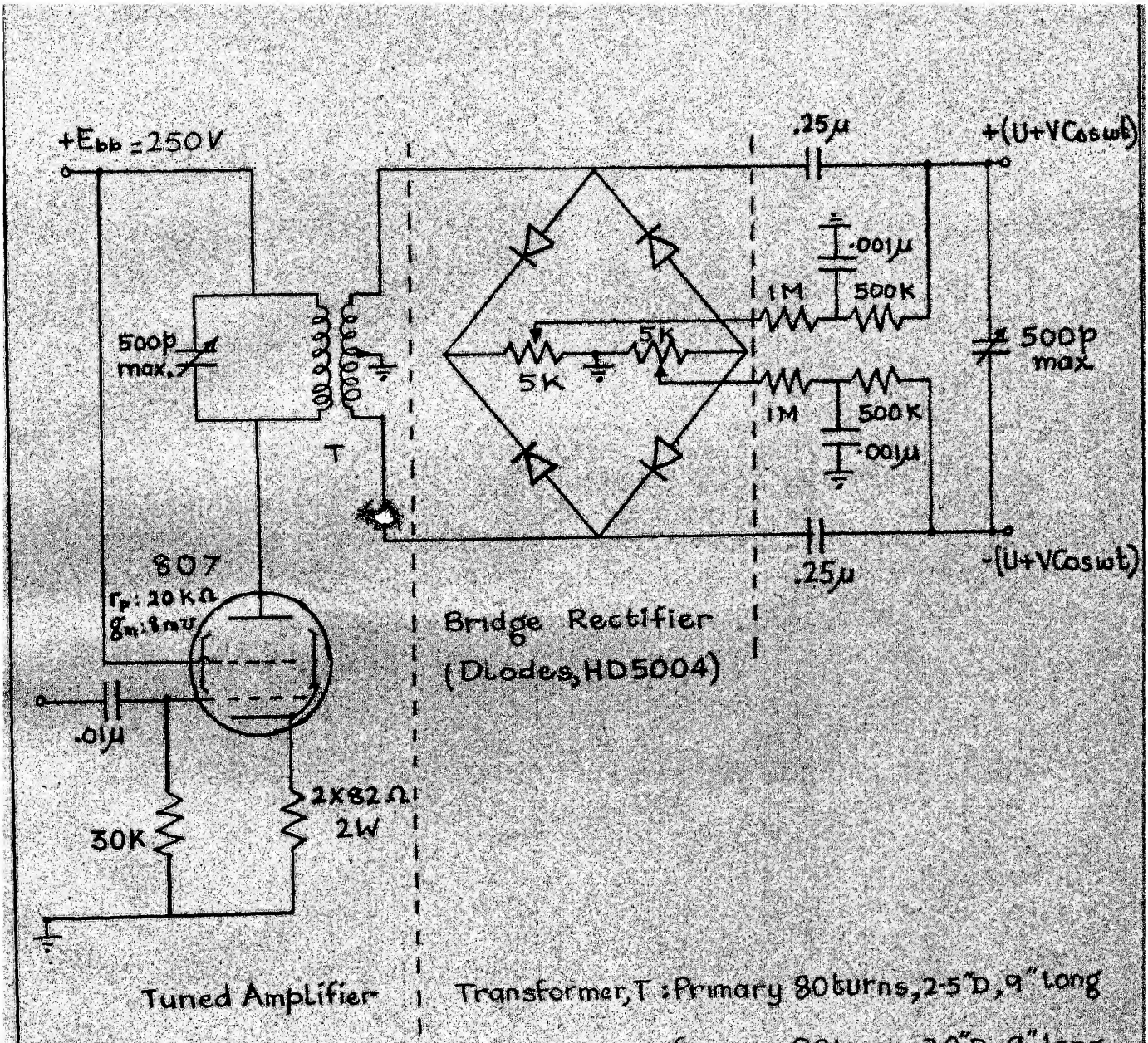

QUADRUPOLE DRIVE CIRCUIT

FIGURE — 7.1

increasing r.f. which increases from minimum to maximum in a time interval of one QMS mass scan (5 seconds). Therefore, the baddwidth required of the tuned circuits is low, and the corresponding Q of the primary and secondary circuits will be high. The requirement of coils for the tuned circuit is that their self resonance must be high compared to 1 MHz. The coils used have spacing = .125 in. between the adjacent turns to keep the self capacitance low, and therefore self-resonant frequency high.

The measurements on the primary and secondary coils are taken on a Q meter at 1 MHz and listed in Table 7.1.

TABLE 7.1

Tuning Capacity, pF	Q	Inductance	Value, μH
270	100	Primary Inductance, Secondary open, L_p	92
735	-	Primary Inductance, Secondary shorted, L_p'	34
410	125	Secondary Inductance, Primary open, L_s	62

The calculated value of mutual inductance is 60 μH.

The physical dimensions of the coil are listed in Table 7.2.

TABLE 7.2

Coil	Length	Diameter	Number of turns
Primary	10 in.	2.5 in.	80
Secondary	10 in.	2.0 in.	80

7.3 Performance of the Circuit

A measurement is made to determine the constancy of the ratio U/V.

The first measurement is made using thermionic diodes, 6AL5, and a D.C. load of 200 K Ω of the bridge rectifier. This data is given in Table 7.3.

TABLE 7.3

+ V r.m.s. volts	- V r.m.s. volts	+ U d.c. volts	-U d.c. volts	Ratio +U/+V	Ratio -U/-V
50.0	50.5	11.7	11.7	.234	.232
39.2	40.0	9.1	9.1	.232	.228
29.8	30.0	7.0	7.0	.235	.233
19.8	20.0	4.9	4.7	.247	.235
10.2	10.2	2.8	2.5	.275	.245

A second measurement is made using semiconductor diodes, HD5004, and a D.C. load of 10 KΩ of the bridge rectifier. This data is given in Table 7.4.

TABLE 7.4

-V r.m.s. volts	+V r.m.s. volts	-U d.c. volts	+U d.c.volts	Ratio +U/+V(= -U/-V)
7.9	7.0	5.2	5.2	0.743
6.6	6.6	4.9	4.9	0.743
6.1	6.1	4.5	4.5	0.738
5.6	5.6	4.1	4.1	0.733
5.1	5.1	3.7	3.7	0.725
4.6	4.6	3.4	3.4	0.739
4.1	4.1	3.0	3.0	0.732
3.6	3.6	2.6	2.6	0.722
3.1	3.1	2.2	2.2	0.710
2.6	2.6	1.8	1.8	0.694
2.1	2.1	1.4	1.4	0.667
1.6	1.6	1.1	1.1	0.687
1.1	1.1	0.7	0.7	0.636
0.6	0.6	0.3	0.3	0.5

It will be seen from Table 7.4 that the ratio U/V is fairly constant, particularly when amplitude of V is high. At low amplitudes of V, the ratio U/V is low. This is due to the higher forward resistance of the

diode (and hence lower d.c. voltage U) in the detection of low amplitude of V.

In conclusion, this method of obtaining the voltage $\pm$ (U+V Cos ω t) is simple and stable. In a QMS, the voltages are applied to the Analyser as shown in Fig. 2.1. Because the voltage U is derived from V, it is only necessary to vary the amplitude of V to achieve a mass scan.

CHAPTER 8

CONCLUSIONS

The electronic hardware to drive the QMS Analyser has been completely fabricated.

This project was a valuable experience in the problems of circuit layout for r.f. circuits.

REFERENCES

1. W. M. Brubaker, N. W. Bell and F. B. Wiens
   Quadrupole Mass Spectrometer for Atmospheric Studies in the 50 to 90 Kilometer Range.
2. N. W. McLachlan
   Theory and Application of Mathieu - Functions, Oxford, 1947.
3. C. A. McDowell,
   Mass Spectrometry, McGraw Hill Book Company Inc.
4. W. M. Brubaker
   The Quadrupole Mass Filter, Bell and Howell Research Center, Pasadena, California.
5. _____
   Quadrupole Mass Spectrometer, Series 210 ULTEK Residual Gas Analyser.
6. C. E. Woodward and C. K. Crawford
   Development of a Quadrupole Mass Spectrometer, Laboratory for Insulation Research, MIT, Dec.1964.
7. T. R. Viswanathan
   An Analog Multiplier Based on Semiconductor Properties, M. Sc. Thesis, Univ. of Saskatchewan, Saskatoon, Canada, 1961.
8. Joachim Dosse
   The Transistor, Basic Theory and Applications, Van Nostrand (1964).

9. Kundu & Banerji

Transistorized Multiplier and Divider and its Applications, Vol. EC-13, June 1964, No. 3.

10. G. E. Platzer

Using Transistor Circuits to Multiply and Divide, Electronics, April 4, 1966.

11. Raphael Littauer

Pulse Electronics, McGraw Hill.

12. W. Paul, H.P. Reinhard, U. Von Zahn

The Electric Mass Filter as a Mass Spectrometer and Isotope Separator (English Translation), Zeit. fur Physik, Bd. 152, S.143-182 (1958).

13. Erich W. Blauth

Dynamic Mass Spectrometers, Elsevier Publishing Company.

14. Carl-Erik Froberg

Introduction to Numerical Analysis, Addison-Wesley Publishing Company, Inc.

15. J. D. Ryder

Engineering Electronics, McGraw-Hill Book Co. (1964).

16. L. J. Sevin

Field Effect Transistors, Texas Instruments Electronics Series.

Date Due
